



Properties of ZrO₂ Passive Film Formed onto Zr Electrode in 1 M NaOH at Low Voltage

V. D. Jović*^z and B. M. Jović

Center for Multidisciplinary Studies, University of Belgrade, 11030 Belgrade, Serbia

In this paper, results of the potentiodynamic–potentiostatic formation of a homogeneous, passive film of ZrO₂ on a Zr electrode in a 1 M NaOH solution at potentials lower than 4.0 V vs saturated calomel electrode are presented. The properties of such a film were investigated by electrochemical impedance spectroscopy (EIS) measurements. After fitting the EIS results by an appropriate equivalent circuit, the capacitance (C_{pf}) and resistance (R_{pf}), as well as the space charge capacitance (C_{sc}) and space charge resistance (R_{sc}) of this film, were determined. The film was found to become an insulator (IN) at the potentials equal to and/or more positive than 2.0 V. In the potential range 0.8 V < E < 2.0 V, a transition from a semiconducting to insulating behavior (SC-IN) has been recorded. The donor densities (N_{sc}), as well as their flatband potentials (E_{fb}) and their space charge layer (d_{sc}) thickness, were determined from the corresponding Mott–Schottky plots recorded in two potential ranges (0.0 V < E < 0.7 V – SC) and (0.8 V < E < 2.0 V – SC-IN), where the film behaved as an n-type semiconductor. From the potential range of the insulating behavior of the film (IN), its thickness was determined from C_{pf} . © 2008 The Electrochemical Society. [DOI: 10.1149/1.2868759] All rights reserved.

Manuscript submitted August 7, 2007; revised manuscript received December 31, 2007. Available electronically March 11, 2008.

Although the anodic behavior of Zr has been the subject of intensive investigations^{1–14} (not referring to anodizing charging curves), only a few papers have presented the polarization characteristics of Zr in different electrolytes.^{1–3} It was shown in all cases that at potentials more positive than the corrosion potential, passivation of the Zr electrode occurs, attributed to the formation of a ZrO₂ passive film.

The properties of the passive ZrO₂ film were mainly investigated by electrochemical impedance spectroscopy (EIS) or capacitance measurements.^{3–11} In most cases, a ZrO₂ passive film was obtained by anodization at high voltages (up to 300 V). In some cases,^{4–8,10} the capacitance was found to be frequency dependent, while Meisterjahn et al.⁹ reported a frequency-independent capacitance over a wide range of frequencies. It was stated by Patrino et al.⁵ that the frequency dependence of the real component of the impedance “indicates that the system Zr/ZrO₂/electrolyte does not behave as a simple RC series circuit”, and that the oxide is described by a complex dielectric constant. The existence of a bilayered ZrO₂ passive film, composed of a thin, compact inner layer at the electrode surface and a porous outer layer of higher conductivity, has been reported by Pauporte et al.^{6,7} In their first paper,⁶ it was shown that in 0.5 M H₂SO₄ and 0.1 M Na₂SO₄ (pH 9) the impedance of ZrO₂ passive films formed by cycling the voltage from 0 V vs IrO₂ to 300 V vs IrO₂ (sweep rate either 100 or 25 mV s⁻¹) could be fitted by an equivalent circuit composed of a constant phase element (CPE₁) and the solution resistance (R_1) connected in series. However, in 0.1 M NaOH, the transformation from one to two layers occurred at voltages higher than 25 V and a complex equivalent circuit composed of CPE₃ (representing the compact oxide layer), the parallel connection of CPE₂ and R_2 (representing the porous oxide layer), and the solution resistance (R_1) could be used to fit the impedance spectra.⁶ In their second paper,⁷ the ZrO₂ passive film was formed and investigated by EIS measurements in 0.1 M (NH₄)₂B₄O₇. The EIS spectra revealed a bilayer structure (as in the previous paper⁶), but the fitting was performed with an equivalent circuit composed of the serial connection of CPE₃ and R_1 , representing a simplification valid for the high-frequency part of the EIS spectra. Because the impedance of the CPE₃ was written as $Z = 1/A_3(j\omega)^n$, the capacity of the passive film was obtained from the equation

$$C_f = \left[A_3 \left(\frac{1}{R_1} \right)^{n-1} \right]^{1/n} \quad [1]$$

with n varying from 0.92 to 0.99. The thickness of the passive film was calculated using the same equation as the one in this paper (Eq. 4; see the Results and Discussion section), and a linear dependence of the film thickness vs applied voltage was obtained. The characteristic of all these investigations is that the ZrO₂ passive film was formed by cycling the potential from 0 to 300 V and measuring the impedance (or capacitance) at the open-circuit potential at several points on the current density vs voltage curve by stopping the cycling^{4–9} at these points. Bardwell et al.⁸ formed passive oxide films on Zr by applying constant current densities (0.05, 0.5, and 5 mA cm⁻²) in steps to 100 mC cm⁻² in different solutions (borates, pyrophosphates, and sulfates of pH 8.4) and measured the impedance of such films at the open-circuit potential. They found that the impedance of the passive film changed with increasing film thickness, and that the best fit could be obtained by an equivalent circuit consisting of the parallel connection of CPE and R_p connected in series with the solution resistance R_s . The increase of R_p with the time of film exposure to the open-circuit potential was interpreted as “the healing of defects, but not as a thickening of the film”. At the same time, it was found that “the kinetics of the increase of R_p with time due to the healing of defects become slower as the thickness increases”. Huot¹⁰ produced and investigated ZrO₂ films in a 0.1 M LiOH solution as a function of surface preparation and the anodic potential by simultaneously measuring the current ($v = 50$ mV s⁻¹) and the electrode capacitance (1000 Hz, 5 mV) during a single cycle of the voltage between 0 and 12 V vs reference hydrogen electrode. “The actual dependence of C and R on frequency suggested that the Zr/ZrO₂/LiOH system does not behave as an ideal capacitor connected in series with the resistance of the solution”. It was concluded that a passive film of 28 nm thickness is obtained at 12 V vs saturated calomel electrode (SCE), which is a typical insulator. Recently, Chen et al.³ investigated the electrochemical behavior of Zr in a borate buffer solution of pH = 6.94 at 250°C and a pressure of 62 bars by measuring the current, impedance, and capacitance as a function of the potential. Passive oxide films were formed at different potentials for 24 h and their thickness was determined from the capacitance measurements (using the same equation as in Ref. 7; see also the Results and Discussion section), since it was found that the capacitance of such a passive oxide film is practically independent of the frequency at $f > 1$ kHz. The EIS spectra recorded for all passive films revealed well-defined depressed semicircles with a Warburg-like impedance at low frequencies. Assuming that the interfacial capacitance could be obtained from $C = -1/\omega Z''$, and neglecting the contribution of the Helmholtz

* Electrochemical Society Active Member.

^z E-mail: vladajovic@ibiss.bg.ac.yu

Table I. α and GF values for EIS results recorded at different potentials.

E/V	4.0	3.8	3.6	3.4	3.2	3.0	2.8	2.6	2.4	2.2	2.0	1.5	1.3	1.1	0.9	0.7	0.5	0.3	0.1
α	0.98	0.98	0.99	0.99	0.98	0.98	0.98	0.99	0.98	0.98	0.98	0.98	0.98	0.97	0.97	0.97	0.96	0.96	0.96
$GF \times 10^4$	1.7	2.2	36	39	5.1	6.1	7.2	12	18	13	25	12	25	6.9	2.1	7.8	12	27	37

layer capacitance, the measured capacitance was found to be equal to the space charge capacitance, C_{sc} . By direct measurement of Mott–Schottky (MS) plots at a sweep rate of 25 mV s⁻¹, a donor density of the order of 10¹⁷–10¹⁸ cm⁻³ of the n-type semiconducting property of the film was determined, while the shift of the intercepts on the vertical and horizontal axes was explained by the presence of a series combination of the voltage-independent capacitance of the outer insulating layer (C_{ox}) and the space charge capacitance (C_{sc}) of the barrier layer, using a modified MS dependence given by Eq. 17 in Ref 3. An identical equation (Eq. 2 in Ref. 11) was used to explain the semiconducting properties of the ZrO₂ passive film¹¹ formed at 12 V vs SCE in 1 M H₃PO₄. The MS plot was obtained by the same procedure as in Ref. 3, except that the frequency used was 500 Hz (with the same assumption that $C = -1/\omega Z''$). C^{-2} was almost independent of the potential in the region from 0 to 12 V, while at potentials more negative than 0 V, a sharp, linear change in the slope of the C^{-2} vs E dependence was recorded, with a minimum at about -0.6 V and a sudden increase of C^{-2} values at more negative potentials. According to the authors, the existence of this minimum on the MS plot was caused by the interface or surface states.

In the paper by Schweinsberg et al.,¹² anodic passive ZrO₂ films formed potentiodynamically (20 mV s⁻¹) on a polycrystalline Zr electrode in 0.5 M H₂SO₄ were investigated on single grains by anisotropy microellipsometry (AME). The results showed a strong texture dependence of the growth of the passive ZrO₂ film on a polycrystalline Zr electrode.

The photoelectrochemical properties of ZrO₂ films formed on Zr electrodes were investigated by Di Quarto et al.¹³ The measurements were performed in different non-deaerated electrolytes on oxide films formed at the open-circuit potential, as well as on oxide films formed after an additional anodization at 5 V on differently prepared Zr metal surfaces. The photo-electrochemical behavior was interpreted by assuming the formation of a duplex oxide film with the possibility of the presence of a hydrated oxide layer formed after immersion in the solution at the open-circuit potential.

Concerning the growth mechanism of passive ZrO₂ films, there is still some controversy. The most accepted high field mechanism (HFM)¹⁴⁻¹⁷ (until 1976) was recently criticized by Zhang et al.,¹⁸ who pointed out that the point defect mechanism (PDM) provides a better account of the experimental data than the HFM.

In this study, an attempt was made to grow a passive ZrO₂ film in 1 M NaOH electrolyte by combining potentiodynamic and potentiostatic techniques at potentials lower than 4.0 V vs SCE, and to investigate its insulating and semiconducting properties by the EIS technique.

Experimental

All experiments were carried out in a three-compartment standard electrochemical cell at room temperature in an atmosphere of purified nitrogen. Before each experiment, the electrolyte was purged with N₂ for 30 min. The same N₂ atmosphere was maintained over the solution during the experiment to minimize oxygen contamination. A platinum mesh counter electrode and the reference, an SCE, were placed in separate compartments. The latter was connected to the working electrode by a Luggin capillary. All solutions were made from analytical grade NaOH (Merck) and ultrapure UV water (Smart2PureUV, TKA).

Polarization and EIS measurements were performed by a computer-controlled Gamry potentiostat (Reference 600) using the corrosion software DC 105 and the electrochemical impedance software EIS 300.

Contact of the Zr (99.8% Goodfellow) sample (1.0 × 1.0 × 0.2 cm³) with a copper wire on the back side of the electrode was made with a silver conductive epoxy paste (Alfa Aesar); the electrode was sealed in an epoxy resin so that an area of only 1 cm² was exposed to the solution. Once mounted, the electrode was polished first with emery papers (1200, 2400, and 4000) and then with polishing clothes impregnated with alumina down to 0.05 μm (1, 0.3, and 0.05 μm), cleaned in an ultrasonic bath for 10 min (to remove traces of the polishing alumina), thoroughly washed with ultrapure UV water, and transferred to the electrochemical cell, where the polarization and EIS measurements were performed.

A polarization diagram was recorded in 1 M NaOH at a sweep rate of 1 mV s⁻¹ starting from the cathodic limit of -1.05 V and finishing at 4.0 V. At the end of the polarization diagram (4.0 V), the Zr electrode was held at this potential for 1 h for a passive oxide film to grow. After passive oxide film formation, EIS spectra were recorded at different potentials, covering the potential range 0.0 V < E < 4.0 V, starting from the upper limit and finishing at the lower limit. After finishing these measurements, EIS spectra at certain potentials in the range 0.0–4.0 V (exactly at 0.0, 0.5, 1.0, 2.0, 3.0, and 4.0 V) were recorded again to determine whether the properties of the passive film changed during this procedure. It was found that the maximum difference between the first and repeated experiments was in the range of ±5%, confirming that the properties of the passive film remained the same during the impedance measurements. The EIS spectra recorded in the potential range 0.6 V < E < 4.0 V were obtained in the frequency range from 0.1 Hz to 10 kHz or 40 kHz, while the EIS spectra at lower potentials were obtained in the frequency range from 0.01 Hz to 40 kHz (the ac amplitude was 10 mV). The EIS spectrum recorded at 0.7 V was repeated in the frequency range from 0.01 Hz to 100 kHz.

In the case of Gamry software (used for fitting the experimental impedance diagrams), “goodness of fit” is the parameter which defines the precision of the fitting. The goodness of fit is similar to Boukamp’s chi-squared. It is a mathematical quantification of how close the experimental points are to the line fitted by complex non-linear least-squares analysis and is represented by the relation (chi-squared)/number of points. The smaller the value, the better the fit, with the value of the goodness of fit 1×10^{-4} for the best fit. In our case, this value was between 1.67×10^{-4} and 3.91×10^{-3} and is given in Table I for several potentials.

Four experiments were repeated on the same sample of Zr electrode with the same procedure of sample surface preparation (polishing) and ZrO₂ film formation, and an average response (the variation of results was ±4%) is presented in the paper.

Results and Discussion

Polarization diagram.— The polarization diagram recorded in 1 M NaOH is shown in Fig. 1. The diagram is characterized by a corrosion potential at about -0.9 V followed by a sharp increase of the current density from about 10⁻⁹ to about 10⁻⁵ A cm⁻² and a current density plateau at this value up to about 0.5 V. A sharp increase in the current density with a peak at about 1.0 V and a current density maximum at about 2×10^{-4} A cm⁻² and another current density plateau (at about 1.5×10^{-4} A cm⁻²) characterize the polarization diagram at more positive potentials. As can be seen in Fig. 1, after holding the electrode at 4.0 V for 1 h, the current density dropped to about 8×10^{-5} A cm⁻².

There are only a few papers reporting the polarization characteristics of Zr electrode in different solutions. In two of them,^{1,2} the

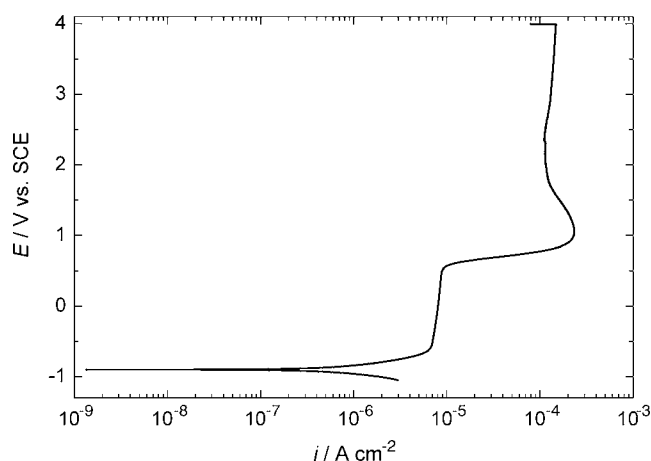


Figure 1. Polarization diagram recorded on a Zr electrode at a sweep rate of 1 mV s^{-1} in 1 M NaOH solution by holding the potential at 4.0 V for 1 h .

polarization characteristics of Zr were presented in the potential range -0.5 to 2.0 V vs SCE in $0.5 \text{ M H}_2\text{SO}_4$, while in another paper³ the polarization characteristics of Zr were presented in the potential range -0.7 to 1.1 V vs standard hydrogen electrode (SHE) in $0.1 \text{ M B(OH)}_3 + 0.001 \text{ M LiOH}$. In all cases, the polarization curves were characterized by a passive region at potentials more positive than the corrosion potential, with some increase of the current density (peak) at a potential of about 1.3 V in $0.5 \text{ M H}_2\text{SO}_4$. The passive region was attributed to the formation of a ZrO_2 film. Figure 1 shows that a similar behavior was recorded in 1 M NaOH , with the first current density plateau between about -0.8 and about 0.5 V . With a further increase of the potential, the current density again increased, followed by a passive region up to 4.0 V , indicating that a new process occurred at the passive ZrO_2 film. Because a breakdown of the passive film on Zr was found not to occur up to 300 V ,⁶ this current density increase could be attributed to further oxidation of the passive ZrO_2 layer, but not to oxygen evolution, because such a process was not detected in the investigated potential region (it should be characterized by much higher current densities). Hence, on holding the potential at 4.0 V for 1 h , further oxidation of ZrO_2 occurred at the electrode surface, followed by a slight decrease of the current density.

EIS results and MS plot analysis.— Some of the Z' – Z'' diagrams recorded at different potentials in the potential range $0.7 \text{ V} < E < 4.0 \text{ V}$ are presented in Fig. 2a, while some of the Z' – Z'' diagrams recorded at different potentials in the potential range $0.0 \text{ V} < E < 0.5 \text{ V}$ are presented in Fig. 2b (experimental points are given as squares, circles, triangles, etc., while the fitting curves are presented as solid lines). The fitting was performed with the equivalent circuit shown in Fig. 3, composed of a resistance (R_{pf}) and a CPE_{pf} connected in parallel (representing the passive film impedance), with the solution resistance (R_s) in series with them. The fitting parameters R_{pf} (R_{sc}), C_{pf} (C_{sc}) are presented in Fig. 4a and 5b, respectively, while the α values and the goodness of fit (GF) are given in Table I for several potentials. As can be seen, all Z' – Z'' diagrams are characterized by well-defined semicircles, and in all cases very good fits were obtained, indicating that the total electrode impedance is dominated by the impedance of the passive oxide film, and that the contribution of the double-layer capacity can be neglected. A small dissipation of points does exist in some cases at lower frequencies, giving a higher value of the GF, up to about 3.9×10^{-3} (see GF in Table I). Taking into account that an ideal GF value amounts to 1×10^{-4} , and that the total measured impedance varies from about 12 to about $10 \text{ M}\Omega \text{ cm}^2$, all fits are satisfactory.

In order to obtain the dimensionally correct value for the capacitance, the following equation was used¹⁹

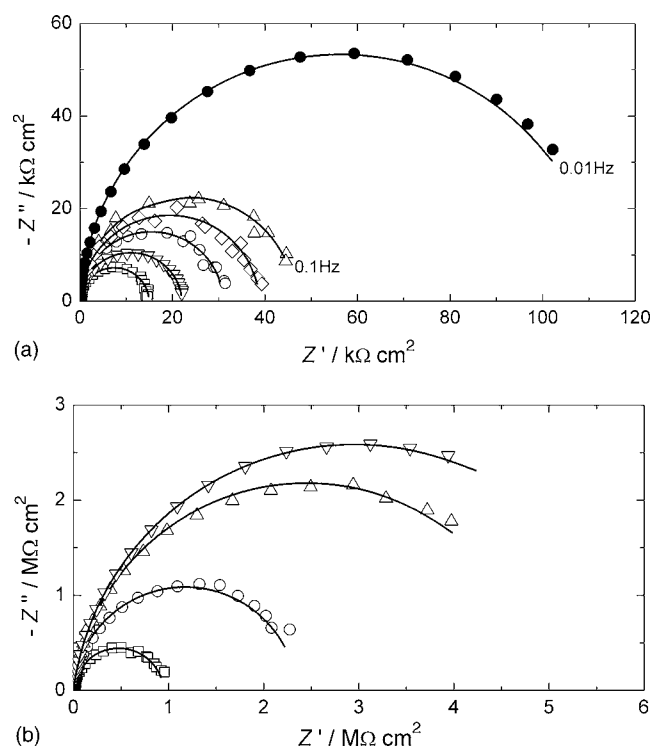


Figure 2. (a) Z' – Z'' diagrams recorded in 1 M NaOH at different potentials (\square : 4.0 V ; \circ : 3.0 V ; \triangle : 2.4 V ; ∇ : 1.0 V ; \diamond : 1.5 V ; \bullet : 0.6 V) for a passive ZrO_2 film. Frequency range: 40 kHz to 0.1 Hz . (b) Z' – Z'' diagrams recorded in the same solution at different potentials (\square : 0.5 V ; \circ : 0.4 V ; \triangle : 0.3 V ; ∇ : 0.2 V). Frequency range: 40 kHz to 0.01 Hz . Experimental points are presented by squares, circles, triangles, etc., while solid lines represent fitting curves.

$$C_{\text{pf}} = [Y_0(R_{\text{pf}})^{1-\alpha}]^{1/\alpha} \quad [2]$$

which is derived from the equation²⁰

$$C_{\text{pf}} = Y_0(\omega_m'')^{\alpha-1} \quad [3]$$

where Y_0 represents the constant in the equation for the constant phase element,²¹ present in all commercially available software (given in $\Omega^{-1} \text{ cm}^{-2} \text{ s}^\alpha$), ω_m'' is the frequency of the maximum of the $-Z''$ vs $\log \omega$ dependence (independent of the value of α) and α is the factor of homogeneity of the space charge distribution in the passive oxide film. It is important to note that in such approach it is assumed that both components of the passive film (C_{pf} and R_{pf}) are dependent on α (these equations^{19,20,22} are generally developed for parallel connection of CPE and R). The frequency dispersion of the capacity as a consequence of the passive film heterogeneity–homogeneity (expressed as α) is closely related to the space charge

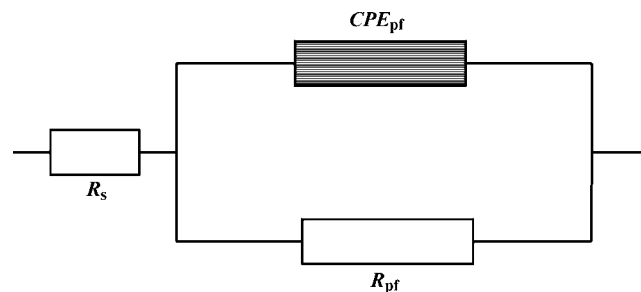


Figure 3. Schematic representation of the equivalent circuit used to fit the experimentally obtained impedance results: R_{pf} : resistance of the passive oxide film; CPE_{pf} : CPE of the passive oxide film; R_s : solution resistance.

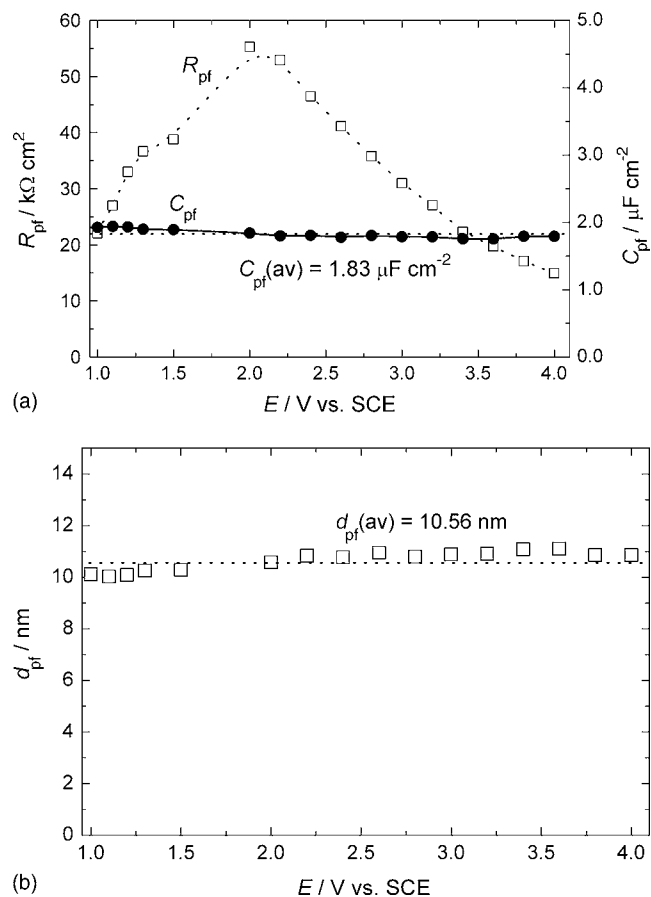


Figure 4. (a) R_{pf} vs E and C_{pf} vs E dependences obtained by fitting $Z'-Z''$ diagrams recorded in the potential range 1.0–4.0 V. (b) Corresponding d_{pf} vs E dependence is obtained using Eq. 4.

distribution in the film; these two parameters are mutually dependent. Such a statement was also pointed out by Van Meirhaege²³ in the analysis of the capacity of semiconductors.²⁴ According to these two references, “the frequency dependence of the capacity must be accompanied by a frequency-dependent parallel resistance.” The parameter α , which defines the homogeneity of the space charge distribution in the passive oxide film, was found to vary between 0.96 and 0.99 (Table I), indicating an almost homogeneous space charge distribution in the oxide film.

After the fitting procedure and calculation of C_{pf} and R_{pf} , these values were used to plot the dependences shown in Fig. 4a. As can be seen, C_{pf} is practically independent of the potential in the potential range 2.0–4.0 V, with the average value being $C_{pf}(av) = 1.83 \mu\text{F cm}^{-2}$. Hence, in this potential region, ZrO_2 behaves as an insulator and accordingly its thickness could be determined by the equation

$$d_{pf} = \frac{\epsilon \epsilon_0}{C_{pf}} \quad [4]$$

where the dielectric constant³ of ZrO_2 is $\epsilon = 22$ and the permittivity of the free space is $\epsilon_0 = 8.85 \times 10^{-14} \text{ F cm}^{-1}$. The results of such calculations, with the average value of the thickness of the ZrO_2 film being $d_{pf}(av) = 10.56 \text{ nm}$, are presented in Fig. 4b. A small increase in the value of C_{pf} could be detected in the potential range 1.0–2.0 V, while C_{pf} (C_{sc}) and R_{pf} (R_{sc}) significantly increase in the potential range 0.0–0.8 V (Fig. 5b).

In order to obtain more detailed information about the semiconducting behavior of the ZrO_2 film, the MS plot was analyzed.

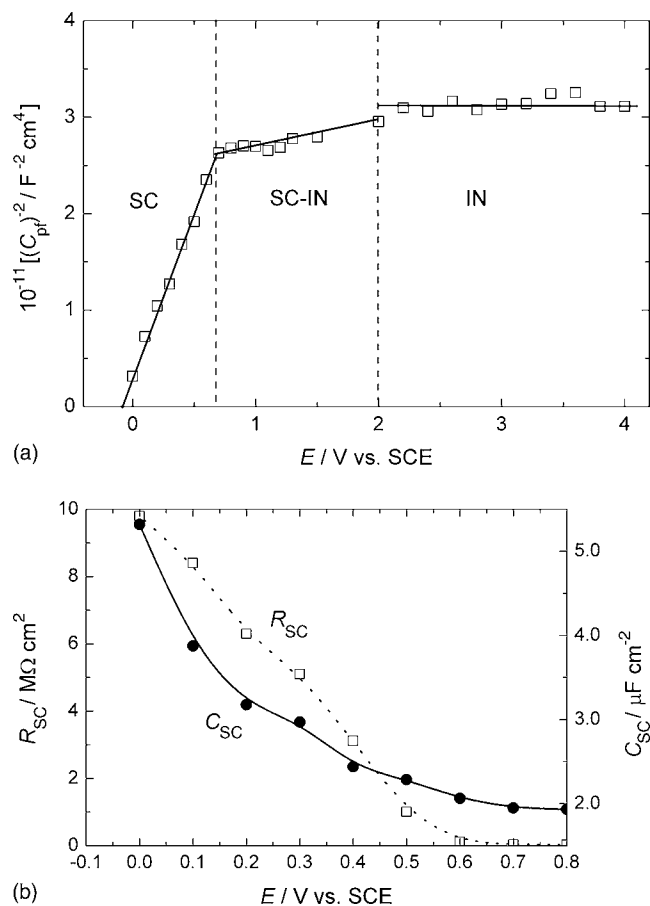


Figure 5. (a) MS plot obtained in the potential range 0.0–4.0 V. (b) R_{sc} vs E and C_{sc} vs E dependences obtained by fitting $Z'-Z''$ diagrams recorded in the potential range 0.0–0.8 V (linear MS plot).

A detailed analysis of the MS plot is shown in Fig. 5a. Three potential regions with different shapes (slope) of the MS plot are detected: an insulating behavior (IN) of the passive film ($E \geq 2.0 \text{ V}$), a transition potential region ($0.7 \text{ V} \leq E \leq 2.0 \text{ V}$) marked with SC-IN, and a space charge region (SC) at potentials $E \leq 0.7 \text{ V}$. From the slope of the SC region ($3.28 \times 10^{11} \text{ F}^{-2} \text{ cm}^4 \text{ V}^{-1}$) of this linear dependence, the donor density of the SC layer, $N_{sc} = 1.96 \times 10^{19} \text{ cm}^{-3}$, was determined, while the flat-band potential, $E_{fb} = -0.1 \text{ V vs SCE}$, represents the intercept on the potential axis. From the slope of the SC-IN region ($0.23 \times 10^{11} \text{ F}^{-2} \text{ cm}^4 \text{ V}^{-1}$) of this linear dependence, the donor density of the SC layer, $N_{sc} = 27.9 \times 10^{19} \text{ cm}^{-3}$, was determined, while the flat-band potential, $E_{fb} = -10.65 \text{ V vs SCE}$, represents the intercept on the potential axis. Both values of the donor density are in a relatively good agreement with the one reported by Meisterjahn⁹ for a zirconium passive film formed at ambient temperature, but they are almost two orders of magnitude higher than the one reported by Chen³ for a zirconium passive film formed in 0.1 M $\text{B(OH)}_3 + 0.001 \text{ M LiOH}$ at an elevated temperature and high pressure ($10^{17}\text{--}10^{18} \text{ cm}^{-3}$). In comparison with the statement of Chen et al.³ that “the film is only lowly-doped with electron donors” (which is most probably the consequence of a low value for potentials used for the passive film formation in Ref. 3, 0.3–0.6 V vs SHE), it is obvious that the films formed at potentials equal to and/or more positive than 2.0 V in 1 M NaOH are highly doped, and that the level of doping increases as the potential region of insulating behavior ($E \geq 2.0 \text{ V vs SCE}$) is approached.

Concerning the value of the flatband potential, there is a discrepancy between our results and the results cited in the literature. In

Morrison's book,²⁴ the value of the flatband potential for ZrO₂ is given as -1.8 V vs SHE, taken from three cited references²⁵⁻²⁷ (Table V.1. on p. 183). After an inspection of citations in the book,²⁴ we found that two of these references (Ref. 26 and 27) do not correspond to the properties of ZrO₂. In Ref. 26, the value of the flatband potential for ZrO₂ is given in Table II, being -1.0 V vs SHE (not -1.8 V vs SHE), and was taken from Ref. 25, while in Ref. 27, the properties of YFeO₃ were investigated and ZrO₂ was not even mentioned. In Ref. 25 the data concerning the flatband potential for ZrO₂ do not exist, except for the diagram with the intensity of the photocurrent as a function of potential (Fig. 2), where the intercept on the potential axis for a ZrO₂ film formed at 8 V vs SCE (no data about the time of anodization) was about -1.5 V vs SCE. As stated in Morrison's book²⁴ (p. 135), "any other unknown voltage sources located outside the semiconductor space charge region such as IR drop or a battery will shift the voltage axis by the amount of the voltage, and appear as a shift in E_{fb} . A common source of such an unknown voltage is a separate phase, a film, on the surface." Hence, one of the reasons could be an additional ohmic resistance, either from the electrode contact or from the cell construction which could cause very negative values of E_{fb} . Considering Ref. 3 and 11, after assuming simplification of the system by a serial connection of the resistance and capacitance, the MS plots show extremely negative values of E_{fb} and, in order to explain such a behavior, the authors had to assume the existence of a duplex oxide film, with the properties of the second oxide film, C_{ox} , being undefined. In this paper it has been shown that such a simplification could give wrong results, even for very homogeneous films (see further discussion).

The thickness of the SC layer (d_{sc}) is calculated by the equation^{28,29}

$$d_{sc} = \left[\frac{2\epsilon\epsilon_0}{eN_{sc}} \left(E - E_{fb} - \frac{kT}{e} \right) \right]^{1/2} \quad [5]$$

where E is the potential of the passive oxide film formation, while e , k , and T have their usual meaning. In the case of the semiconducting potential region (SC), the value of E was 0.8 V, the first point where this oxide film behaves differently; the change of the slope on the MS plot (see Fig. 5a). In the case of the transition potential region (SC-IN) this value was 2.0 V, the first point where this oxide film behaves as an insulator. By the analysis of the MS plot recorded in the SC-IN region in Fig. 5a, an extremely negative and unrealistic value for the E_{fb} was obtained ($E_{fb} = -10.65$ V vs SCE), but the thickness of the SC layer (calculated using Eq. 5) remained practically the same as the one recorded for the semiconducting (SC) region [$d_{sc}(\text{SC}) = 10.4$ nm, $d_{sc}(\text{SC-IN}) = 10.0$ nm] and was practically identical to the thickness of the insulating oxide film [$d_{pf}(\text{av}) = 10.56$ nm]. Such a behavior indicates that in the transition potential region it is possible to obtain linear MS plots with the reasonable values for the donor densities. Extremely negative values for E_{fb} could be explained either by the introduction of a duplex oxide film, as it was the case in Ref. 3 and 11, or by the presence of the transition potential region. Taking into account that the values of d_{sc} and $d_{pf}(\text{av})$ are practically identical and that there is no indication of the presence of a second semicircle (corresponding to another oxide layer) in the EIS results (Fig. 2), it appears that the assumption of the existence of a duplex oxide film is unrealistic for this case.

According to Morrison,²⁴ by changing the cell voltage the experiment can produce four different forms of the SC layer. One of them is a depletion layer, sometimes termed an exhaustion layer. This layer forms if the majority carriers are extracted in moderate amounts, the surface region is "depleted" of majority carriers, and minority carriers are not present, thus the surface region is depleted (exhausted) of both forms of mobile carriers. In such a case, the surface region is essentially insulating. Hence, it is most likely that with an increasing potential such a process occurs in the semicon-

ducting oxide, resulting in the formation of an insulator, because the thickness of the SC layer (d_{sc}) is practically identical to the thickness of the passive oxide film [$d_{pf}(\text{av})$].

The impedance of the process occurring in the semiconducting oxide film could be represented by the parallel connection of C_{pf} and R_{pf} (see Fig. 6a and c) or the serial connection of C_{pf} and R_s (see Fig. 6b and d), respectively. The simplification of the process occurring at the semiconducting electrodes, assuming either the serial connection of C_{pf} and R_s or the parallel connection of C_{pf} and R_{pf} (with C_{pf} being a parallel plate capacitor), is very often used in the literature.^{3,11,30-35} In the case of the serial connection of C_{pf} and R_s , the capacitance is calculated directly from the value of Z'' , i.e., $C_{pf} = 1/2\pi fZ''$, while in the case of the parallel connection of C_{pf} and R_{pf} , the capacitance is calculated directly from the value of Y'' , i.e., $C_{pf} = Y''/2\pi f$. The results of such an analysis (C_{pf} vs E) are presented in Fig. 6 for different frequencies (\square : 10 kHz; \circ : 1 kHz; \triangle : 100 Hz, and ∇ : 10 Hz) for the passive ZrO₂ film in the potential range 0.9–4.0 V (Fig. 6a and b, insulating behavior) and in the potential range 0.0–0.7 V (Fig. 6c and d, semiconducting behavior). As can be seen in all cases, for frequencies higher than 10 Hz, C_{pf} is practically independent of potential, and well-defined linear C_{pf} vs E plots are obtained. For the potential range 0.9–4.0 V (Fig. 6a and b, insulating behavior), this is in accordance with the plots presented in Fig. 4a, but the values of C_{pf} were found to depend on the frequency for both the assumption of the serial connection of C_{pf} and R_s and the parallel connection of C_{pf} and R_{pf} . Moreover, neither of the average C_{pf} values matches the one obtained from Fig. 4a. At the same time, for the potential range 0.0–0.7 V (Fig. 6c and d, semiconducting behavior), instead of the C_{pf} vs E plot presented in Fig. 5b, linear C_{pf} vs E plots independent of potential were obtained (except for $f = 10$ Hz). It is most likely that the change of the values of C_{pf} as a function of the frequency is the consequence of the fact that the passive film capacitance is not exactly a parallel plate capacitor, but is represented by the CPE and, although the values of α are close to unity (0.96–0.99), the values of C_{pf} are sensitive to such small deviations from unity. Usually such an approach is used^{3,11,30-35} at only one constant frequency (1 kHz in most cases), assuming that, at such a particular frequency, the system could be described by the serial connection of the solution resistance and oxide film capacitance (neglecting the contribution of the double-layer capacitance). This is a correct assumption, but, for impedance spectra of almost all electrochemical systems, this assumption (simplification) is valid and the question arises as to whether the obtained values for the donor density and the flatband potential are correct. In this paper it is shown that such an assumption can lead not only to the wrong values, but also to a different dependence of the passive film capacity on frequency (Fig. 6). Hence, according to the results presented in this work, it appears reasonable to avoid direct MS (or C_{pf} vs E) plots and obtain correct values of C_{pf} by fitting EIS results and then plotting the corresponding MS (or C_{pf} vs E) dependences.

Conclusions

This paper showed that a homogeneous passive ZrO₂ film could be formed on a Zr electrode in 1 M NaOH by a combination of potentiodynamic and potentiostatic techniques at potentials more negative than 4.0 V vs SCE. The film was found to become insulator (IN) at the potentials equal to and/or more positive than 2.0 V as a result of a depletion (exhaustion) layer formation. In the potential range 0.8 V < E < 2.0 V, a transition from a semiconducting to insulating behavior (SC-IN) has been recorded. The donor densities (N_{sc}), as well as their flatband potentials (E_{fb}) and their thicknesses of the SC layer (d_{sc}), were determined from the corresponding MS plots recorded in two potential ranges (0.0 V < E < 0.7 V – SC) and (0.8 V < E < 2.0 V – SC-IN), where film behaved as an n-type semiconductor. It was also shown that it seems reasonable

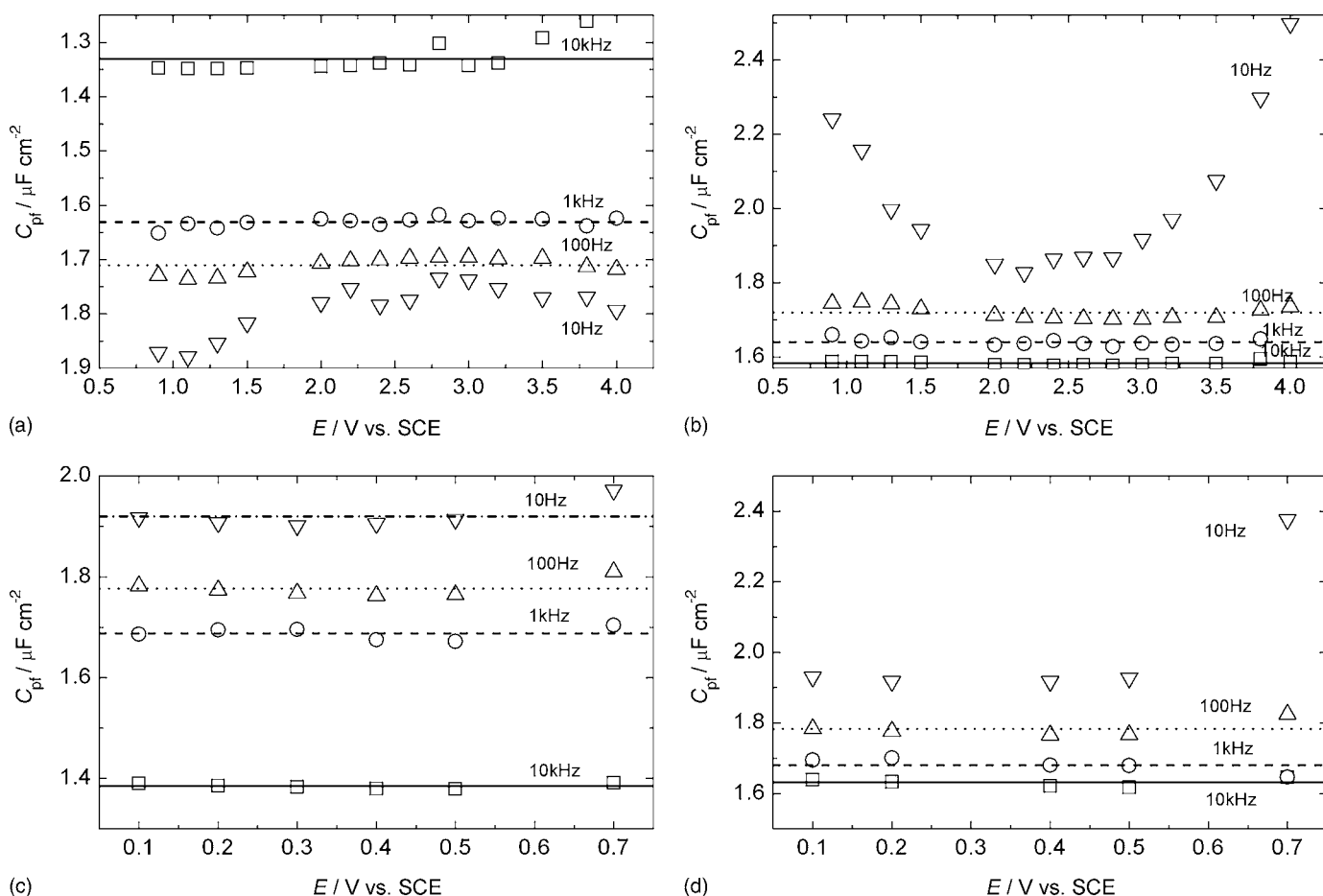


Figure 6. (a and c) C_{pf} vs E dependences obtained by the analysis of EIS results for different frequencies (\square : 10 kHz; \circ : 1 kHz; \triangle : 100 Hz; and ∇ : 10 Hz) assuming a parallel connection of C_{pf} and R_{pf} . (b and d) C_{pf} vs E dependences obtained by the analysis of EIS results for different frequencies (\square : 10 kHz; \circ : 1 kHz; \triangle : 100 Hz; and ∇ : 10 Hz) assuming a serial connection of C_{pf} and R_s .

to avoid direct MS (or C_{pf} vs E) plots and obtain correct values of C_{pf} by fitting the EIS results and then plotting the corresponding MS (or C_{pf} vs E) dependences.

References

- D. Q. Peng, X. D. Bai, X. W. Chen, Q. G. Zhou, X. Y. Liu, and R. H. Yu, *Appl. Surf. Sci.*, **227**, 73 (2004).
- D. Q. Peng, X. D. Bai, X. W. Chen, Q. G. Zhou, X. Y. Liu, and R. H. Yu, *Appl. Surf. Sci.*, **221**, 259 (2004).
- Y. Chen, M. Urquidí-Macdonald, and D. D. Macdonald, *J. Nucl. Mater.*, **348**, 133 (2006).
- F. Di Quarto, S. Piazza, and C. Sunseri, *J. Electrochem. Soc.*, **130**, 1014 (1983).
- E. M. Patrito, R. M. Torresi, E. P. M. Leiva, and V. A. Macagno, *J. Electrochem. Soc.*, **137**, 524 (1990).
- T. Pauporte and J. Finne, *J. Appl. Electrochem.*, **36**, 33 (2006).
- T. Pauporte, J. Finne, A. Kahn-Harari, and D. Lincot, *Surf. Coat. Technol.*, **199**, 213 (2005).
- J. A. Bardwell and M. C. H. McKubre, *Electrochim. Acta*, **36**, 647 (1991).
- P. Meisterjahn, H. W. Hoppe, and J. W. Schultze, *J. Electroanal. Chem. Interfacial Electrochem.*, **217**, 159 (1987).
- J.-Y. Huot, *J. Appl. Electrochem.*, **22**, 852 (1992).
- A. Goossens, M. Vazquez, and D. D. Macdonald, *Electrochim. Acta*, **41**, 35 (1996).
- M. Schweinsberg, A. Michaelis, and J. W. Schultze, *Electrochim. Acta*, **42**, 3303 (1997).
- F. Di Quarto, S. Piazza, C. Sunseri, M. Yang, and S.-M. Cai, *Electrochim. Acta*, **41**, 2511 (1996).
- T. P. Hoar, in *Modern Aspects of Electrochemistry*, Vol. 2, J. O'M. Bockris, Editor, Academic Press, New York (1959).
- M. J. Dignam, in *Oxides and Oxide Films*, Vol. 1, J. W. Diggle, Editor, Marcel Dekker, New York (1973).
- A. K. Vijh, *Electrochemistry of Metals and Semiconductors*, Marcel Dekker, New York (1973).
- A. T. Fromhold, Jr., in *Oxides and Oxide Films*, Vol. 3, J. W. Diggle and A. K. Vijh, Editors, Marcel Dekker, New York (1976).
- L. Zhang, D. D. Macdonald, E. Sikora, and J. Sikora, *J. Electrochem. Soc.*, **145**, 898 (1998).
- http://www.gamry.com/App_Notes/PDF/jovic.pdf, p. 1 (2003) last accessed July 10, 2007.
- C. H. Hsu and F. Mansfeld, *Corrosion (Houston)*, **57**, 747 (2001).
- J. R. Macdonald, *Impedance Spectroscopy Emphasizing Solid Materials and Systems*, Wiley, New York (1987).
- M. E. Orazem, P. Shukla, and M. A. Membrino, *Electrochim. Acta*, **47**, 2027 (2002).
- R. L. Van Meirhaeghe, E. C. Dutiot, F. Cardon, and W. P. Gomes, *Electrochim. Acta*, **20**, 995 (1975).
- S. R. Morrison, *Electrochemistry at Semiconductor and Oxidized Metal Electrodes*, Plenum Press, New York (1980).
- O. P. Clechet, J. Martin, R. Oliver, and C. Vallony, *C. R. Seances Acad. Sci., Ser. C*, **282**, 887 (1976).
- H. H. Kung, H. S. Jarret, A. W. Sleight, and A. Ferretti, *J. Appl. Phys.*, **48**, 2463 (1977).
- M. A. Butler, D. S. Ginley, and M. Eibschutz, *J. Appl. Phys.*, **48**, 3070 (1977).
- V. A. Alves and C. M. A. Brett, *Electrochim. Acta*, **47**, 2081 (2002).
- V. D. Jović, M. W. Barsoum, B. M. Jović, A. Ganguly, and T. El-Raghy, *J. Electrochem. Soc.*, **153**, B238 (2006).
- E. Sikora and D. D. Macdonald, *J. Electrochem. Soc.*, **147**, 4087 (2000).
- E.-J. Lee and S.-I. Pyun, *J. Appl. Electrochem.*, **22**, 156 (1992).
- S. Kudelka and J. W. Schultze, *Electrochim. Acta*, **42**, 2817 (1997).
- W. P. Gomes and D. Vanmaekelbergh, *Electrochim. Acta*, **41**, 967 (1996).
- J. Sikora, E. Sikora, and D. D. Macdonald, *Electrochim. Acta*, **45**, 1875 (2000).
- E. Sikora and D. D. Macdonald, *Electrochim. Acta*, **48**, 69 (2002).